JOURNAL OF CATALYSIS 85, 105–116 (1984)

Kinetics of the Methanation of Carbon Monoxide on an Alumina-Supported Nickel Catalyst

J. KLOSE AND M. BAERNS

Lehrstuhl für Technische Chemie, Ruhr-Universität Bochum, Postfach 102148, D-4630 Bochum, West Germany

Received March 4, 1983; revised July 4, 1983

The kinetics of the methanation of carbon monoxide has been investigated on an alumina-supported nickel catalyst having an average particle size of 1.2 mm. The following experimental conditions were applied: $0.001 \leq p_{CO} \leq 0.6$ bar, $1 \leq p_{H_2} \leq 25$ bar, $453 \leq T \leq 557$ K. The kinetics can be satisfactorily explained by assuming equilibrium of dissociative carbon monoxide and hydrogen adsorption and hydrogenation of surface carbon to a CH_2-species involving two adsorbed hydrogen atoms as the rate limiting step:

$$r_{CH_4} = \frac{k_{CH_2} K_C K_H{}^2 p_{CO}{}^{0.5} p_{H_2}}{(1 + K_C p_{CO}{}^{0.5} + K_H p_{H_2}{}^{0.5})^3}$$

Both the hydrogenation of the surface oxygen to water and of the CH_2-species to methane are considered to be fast processs. The formation of ethane, which occurred to a small extent, could be described by a kinetic model which tentatively postulates the dimerization of the CH_2-species to an alkyl carbenic surface species and its consecutive hydrogenation.

INTRODUCTION

For the methanation of carbon monoxide two basic mechanisms have been suggested in the past. On the one hand, some researchers such as Vlasenko and Yuzefovich (*1*) and Vannice (*2*) have postulated that reaction occurs between molecularly adsorbed carbon monoxide and hydrogen via C/H/O-intermediates. On the other hand, according to more recent evidence (*3–13*), dissociative adsorption of carbon monoxide and hydrogen followed by reaction between surface carbon and hydrogen atoms via CH_x-species appears to be more likely. Based on these two mechanisms various rather divergent kinetic models have been derived. However, careful analysis (*14*) shows that the range of conditions investigated, particularly with respect to the partial pressures of carbon monoxide and hydrogen, was often too small to discriminate between the models. Furthermore, suspicion seems justified that some of the earlier results have been disguised by pore diffusion within the catalyst. Recently a very comprehensive and careful kinetic study (*15*) has been published from which valuable conclusions can be drawn, but the present work leads to a different kinetic model with respect to the rate determining step, as will be discussed later.

The objective of this work was to investigate the methanation kinetics of carbon monoxide over a wide range of partial pressures of carbon monoxide and hydrogen as well as temperature, to derive a suitable kinetic equation, and to obtain new indications about the reaction mechanism.

EXPERIMENTAL

Method of investigation. The kinetic measurements were performed in a continuously operated gradientless recycle reactor under conditions such that it behaved as a perfectly mixed stirred tank reactor. Therefore the reaction rates could be derived from the difference between inlet and outlet streams of a key component. The rates could be assigned to the partial pres-

0021-9517/84 $3.00

sures of the reactants prevailing in the reactor. Based upon the two basic reaction mechanisms mentioned above, kinetic models were derived applying the principle of one rate-determining step and assuming that the adsorption of the kinetically relevant species can be described by Langmuir adsorption isotherms. The only ones considered were those which were able to describe qualitatively the experimentally observed relationships between the rates of formation of methane and the partial pressures of the reactants. The resulting kinetic models are summarized in the following general equation:

$$r_{CH_4} = \frac{kK_1K_2p_{CO}{}^x p_{H_2}{}^y}{(1 + \sum_i K_i p_i{}^w)^z} \qquad (1)$$

The parameters k and K_i of Eq. (1) were estimated for 15 models with different exponents x,y,z and various combinations of the adsorption terms $K_ip_i{}^w$ within each model. The various combinations of the exponents and of the rate-determining steps (rds) are listed in Table 1. Furthermore, models 10 to 15 assume an irreversible step in the formation of water, which is not considered to be the limiting step for the overall rate. The coverage of the surface with oxygen is supposed to be low according to results from Goodman *et al.* (*9*), who found only carbon and no oxygen on an active nickel catalyst surface by AES analysis, i.e., the adsorbed O- or OH-species are not the most abundant surface intermediates.

For parameter estimation a nonlinear regression procedure was applied, which uses a modified Gauss–Newton method (*16*). The resulting model equations were subjected to various statistical tests: the variance, the standard deviation of the model parameters and the deviations between measured and calculated reaction rates were taken as criteria for model discrimination.

The variances of all models, of which parameters could be estimated, were tested against the variance of the best model on a 99% level of significance by the F-test (*17*). Models showing standard deviations over 100% in the parameters were rejected. Furthermore, on a 95% level of significance the symmetric Williams–Kloot test (*17*) was applied to models passing the F-test; hereby it is tested whether an assumed model describes the observed reaction rates better than another model with respect to the deviations between measured and calculated values.

Catalyst. A commercial nickel (18 mass%) catalyst supported on alumina (RCH 18/10 supplied by Ruhrchemie AG, Oberhausen) was used. This was crushed to

TABLE 1

Kinetic Models According to Eq. (1) Considered for Discrimination

Model	Rate determining step[a]	Exponents of Eq. (1)		
		x	y	z
1	*CO + *H_2	1	1	2
2	*CO + *H	1	0.5	2
3	*CO + 2*H	1	1	3
4	*CHO + *H_2	1	1.5	2
5	*CHO + *H	1	1	2
6	*CHO + 2*H	1	1.5	3
7	*CHOH + *H_2	1	2	2
8	*CHOH + *H	1	1.5	2
9	*CHOH + 2*H	1	2	3
10	*C + *H *O + *H	0.5	1	2
11	*C + 2*H *O + 2*H	0.5	1	3
12	*C + *H *O + *H	0.5	0.5	2
13	*C + *H *OH + *H	0.5	0.75	2
14	*CH + *H *O + *H	0.5	0.75	2
15	*CH + *H *OH + *H	0.5	1	2

[a] For models 10 to 15 the assumed irreversible step in the formation of water is also given.

TABLE 2

Physical Properties of the Reduced Catalyst

ρ_{cat} (g cm^{-3})	S_{BET} (m^2 g^{-1})	r_{pore}[a] (nm)	S_{Nickel} (m^2 g^{-1})
1.33	169	4.1	ca. 14

[a] Mesopores between 1.5 and 50 nm.

particle sizes of 1.0 to 1.4 mm in order to avoid pore diffusion effects. The catalyst was reduced by hydrogen (99.999%) at 1 bar and 623 K during 17 h (space velocity = 2000 liters (STP)/h liter catalyst). The physical properties determined for the reduced catalyst are listed in Table 2.

During the kinetic measurements the catalyst deactivated; this process was followed by determining at reference conditions (p_{CO} = 0.2 bar, p_{H_2} = 9.6 bar, T = 485 K) the rate of methane formation r^{ref} after various experimental conditions had been established. The relationship between r^{ref} and operating time is shown in Fig. 1. If one assumes that only the number of active sites is diminished by deactivation, the reaction kinetics and the deactivation kinetics are separable. This view was supported by the fact that based on the kinetic model obtained in this work (compare Eq. (2)) the ratio of the kinetic rate constants k_{CH_2} determined at different activity levels was equal to the ratio of the respective methanation rates at comparable reaction conditions while the pseudoadsorption constants did not change significantly. Therefore all data points measured at time t were corrected to an activity level at t_0 = 230 h (which corresponds to the end of catalyst conditioning) by the rate of methane formation at reference conditions:

$$r_0 = (r_0^{ref}/r_t^{ref})r_t$$

Procedure. A schematic diagram of the apparatus is shown in Fig. 2. The kinetic measurements were performed by means of a Berty-type recycle reactor (Autoclave Engineers Inc., Erie, Pa.). Carbon monoxide (99.97%), hydrogen (99.99%), and nitrogen (99.99%) were fed by flowmeters at total pressures of 20 or 30 bars. After passing a mixing chamber filled with molecular sieves M13X the gases entered the reactor. The reaction mixture leaving the reactor was cooled to room temperature; hereby most of the water was separated. After reducing the total pressure to 1 bar the remaining proportion of water vapor amounted to about 0.2 vol%; this concentration did not disturb the subsequent analysis of the other products. The gas was ana-

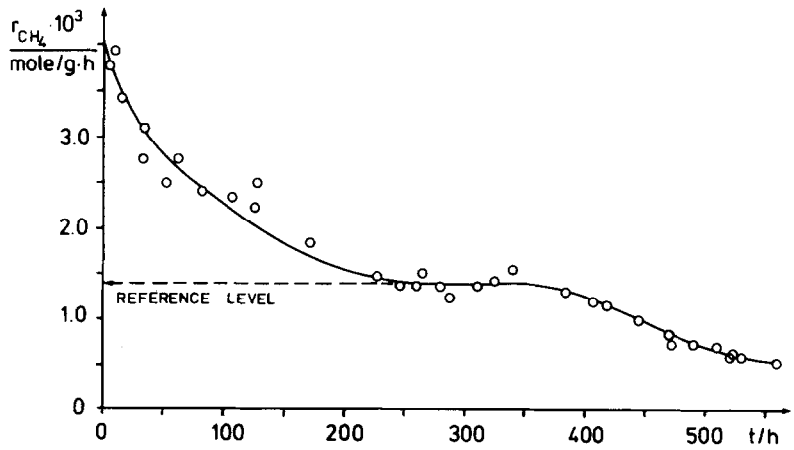

FIG. 1. Effect of operating time on the rate of methane formation measured at reference conditions: T = 485 K; p_{H_2} = 9.6 bar; p_{CO} = 0.2 bar.

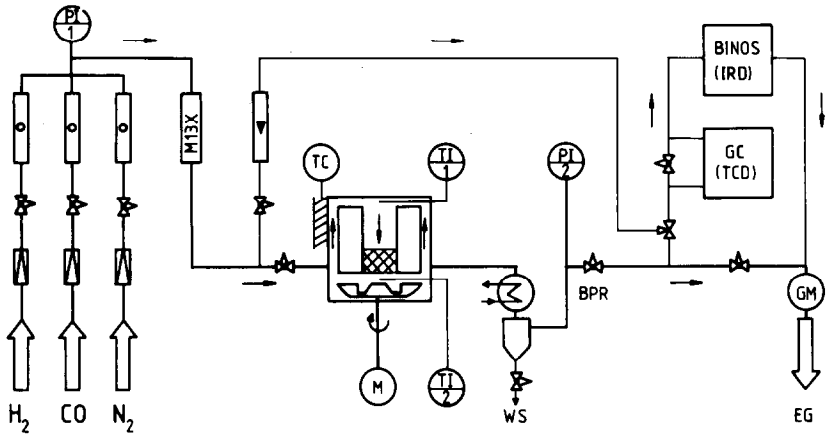

FIG. 2. Schematic diagram of the apparatus used for the kinetic study (BPR, back pressure regulator; GM, gas meter; IRD, infrared detector; TCD, thermal conductivity detector; WS, water separation; EG, exit gas).

lyzed by gas chromatography using a thermal conductivity detector. N_2, CH_4, and CO were separated on a molecular sieve M13X column (d = 0.32 mm, L = 3 m; 30 ml/min helium; temperature program 4°C/min starting from 55 to 100°C); for separation of CO_2, C_2H_6, and higher paraffins a Porapak Q column (d = 0.32 mm, L = 2 m; 30 ml/min helium; 2 min isotherm at 45°C, then temperature program 15°C/min to 200°C) was used. In addition, a continuously operating infrared gas analyzer (BINOS-Leybold Heraeus GmbH, Hanau, W. Germany) was used for determining CO (0–0.3 vol%) and CH_4 (0–1.5 vol%). The analytical error associated with the concentrations generally amounted to ±7%; only at very low concentrations of CO_2 and C_2H_6 was the error higher. The gas analysis was corrected to moist gas conditions in the recycle reactor on the basis of the condensed proportion of water vapor. Further details on the experimental procedure have been reported elsewhere (*14*).

Reaction temperatures applied were 453, 463, 473, 485, 496, and 557 K. Partial pressures of carbon monoxide and hydrogen were varied from 0.001 to 0.6 bar and from 1 to 25 bar, respectively. Under these conditions the ratio of hydrogen and carbon monoxide partial pressures amounted in each experiment to at least 10 to avoid excessive carbon deposition on the catalyst.

RESULTS

Reaction Products

The main products were methane and water. Ethane was found in small concentrations while higher paraffins occurred in traces only. The selectivity of the methane formation based upon the sum of formed hydrocarbons amounted to 80 to 100%; the latter value was nearly reached at high ratios of hydrogen and carbon monoxide or high temperature. The formation of carbon dioxide was negligible. Traces of methanol and ethanol were detected in the condensed water phase. The carbon mass balance amounted in all experiments to more than 95% of the carbon monoxide input.

Dependence of Reaction Rate on Partial Pressures and Temperature

The experimentally determined dependences of the methanation rate upon the partial pressures of hydrogen and carbon monoxide are presented in Figs. 3 to 5; the respective results on ethane formation are shown in Fig. 6. At constant hydrogen partial pressure, the rate of methane formation as a function of carbon monoxide partial

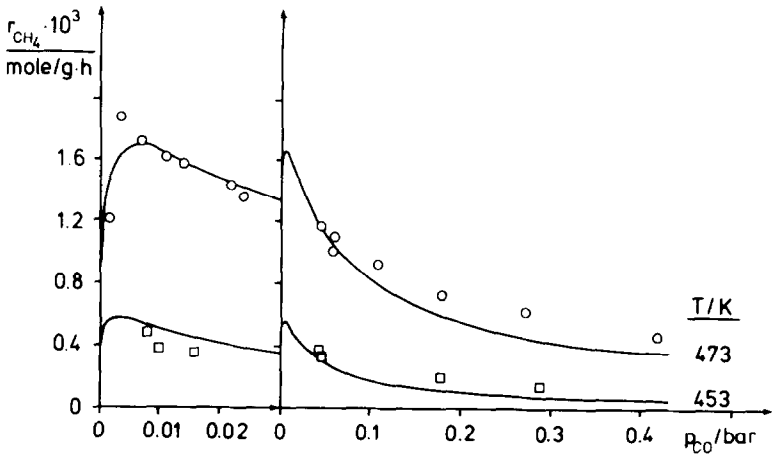

FIG. 3. Rate of methane formation at p_{H_2} = 9.9 bar (symbols show experimental points, lines calculated by Eq. (2)).

pressure passes through a maximum. At constant carbon monoxide partial pressure the rate increases with increasing hydrogen partial pressure. The rate maximum shifts to higher carbon monoxide partial pressures with increasing temperature as well as increasing hydrogen partial pressure. Under the applied reaction conditions, the rate of methane formation is not affected by the partial pressures of water vapor and methane (*14*). The rate of ethane formation increases with increasing carbon monoxide partial pressure; it is slightly decreased by hydrogen partial pressure.

Influence of Heat and Mass Transfer on the Chemical Reaction

By appropriate tests as summarized in Ref. (*18*) the effects of inter- and intraparticle temperature and concentration gradients on the reaction rates were determined. Thus:

(i) Interparticle gradients were smaller than experimental accuracy and hence were neglected.

(ii) No intraparticle temperature gradients occurred.

(iii) Concentration gradients within the

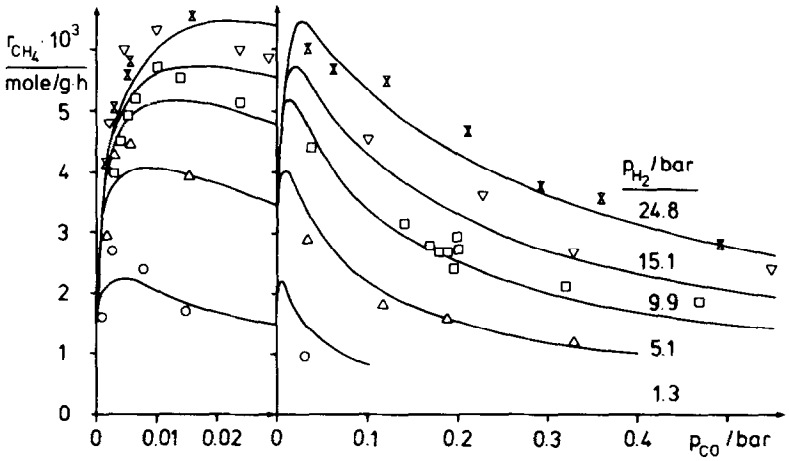

FIG. 4. Rate of methane formation at T = 496 K (symbols show experimental points, lines calculated by Eq. (2)).

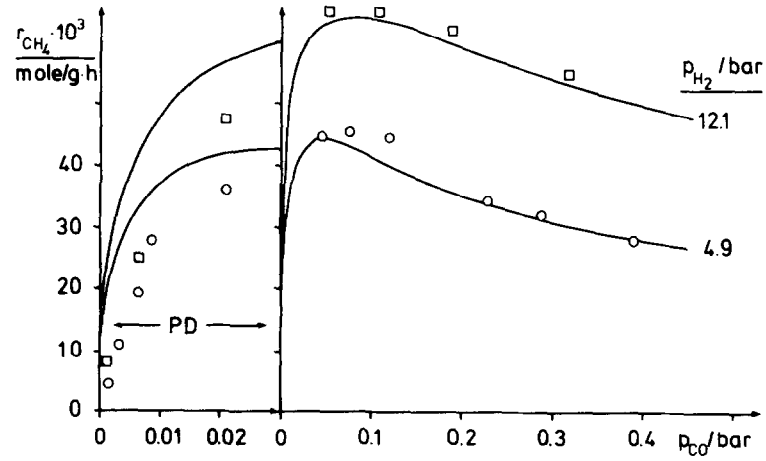

FIG. 5. Rate of methane formation at $T = 557$ K (symbols show experimental points, lines calculated by Eq. (2)) (PD: range of pore diffusion).

catalyst pellet could generally be excluded; only under those conditions where the methanation rate exhibited a maximum as a function of carbon monoxide partial pressure did small gradients exist, especially at higher reaction temperatures (compare Fig. 5).

For evaluation of the various proposed kinetic models the only data used were those for which the modified Thiele modulus was smaller than or equal to 1.7. (A detailed analysis of the interaction of pore diffusion and chemical reaction for carbon monoxide methanation will be presented in a subsequent paper.)

Evaluation of the Kinetic Models

Model discrimination and parameter estimation for the rate equations listed in Table 1 were based on 168 data sets, i.e., combinations of rates of methane formation and reaction conditions. Details on the results of the statistical tests are given elsewhere (*14*). The following rate equation for the methanation of carbon monoxide is considered to be the best on the basis of the statis-

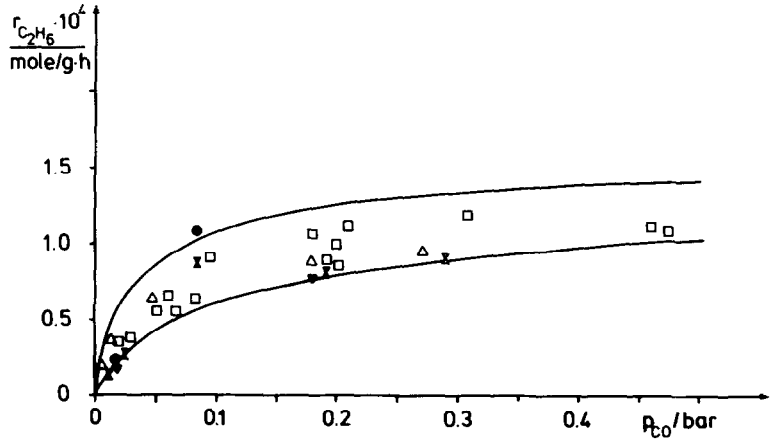

FIG. 6. Rate of ethane formation at $p_{H_2} = 1.1$ (●), 5.1 (△), 9.9 (□), 15.0 (⧖), 18.4 (▼) bar, and $T = 485$ K (symbols show experimental points, lines calculated by Eq. (4): upper line $p_{H_2} = 1.1$ bar, lower line $p_{H_2} = 18.4$ bar).

TABLE 3

Parameters k_i and K_i of the Rate Eqs. (2) and (4) for the Formation of Methane and Ethane, Respectively: $k_i = k_i^0 \exp(-E_i/RT)$; $K_i = K_i^0 \exp(-\Delta H_i/RT)$

$k_{CH_2}^0$ (mol/h g)	E_{CH_2} (kJ/mol)	$k'^0_{C_2H_4}$ (mol/h g)	$E'_{C_2H_4}$ (kJ/mol)
$(4.8 \pm 2.1) \times 10^9$	103 ± 2	$(1.8 \pm 1.7) \times 10^7$	102 ± 4
K_C^0 ($bar^{-0.5}$)	ΔH_C (kJ/mol)	K_H^0 ($bar^{-0.5}$)	ΔH_H (kJ/mol)
$(5.8 \pm 3.8) \times 10^{-4}$	-42 ± 3	$(1.6 \pm 1.3) \times 10^{-2}$	-16 ± 3

tical tests mentioned above:

$$r_{CH_4} = \frac{k_{CH_2} K_C K_H {}^2 p_{CO}{}^{0.5} p_{H_2}}{(1 + K_C p_{CO}{}^{0.5} + K_H p_{H_2}{}^{0.5})^3} \quad (2)$$

This equation agrees rather closely to the one proposed by Rautavuoma and van der Baan (*19*) for the consumption of carbon monoxide during Fischer–Tropsch synthesis catalyzed by cobalt:

$$-r_{CO} = \frac{k p_{CO}{}^{0.5} p_{H_2}}{(1 + K_C p_{CO}{}^{0.5})^3} \quad (3)$$

The only difference between the two rate equations is the fact that Rautavuoma and van der Baan neglected inhibition of the reaction by hydrogen adsorption.

For the above rate Eq. (2) the preexponential factor and the activation energy as well as the pseudoadsorption constants and the respective adsorption enthalpies are summarized in Table 3. The standard deviations of the preexponential factors are high because they are strongly affected by only small changes in the activation energy E and enthalpies of adsorption ΔH, respectively.

The agreement of measured and calculated methanation rates is satisfactory over the whole range of experimental conditions investigated, as is shown in Figs. 3 to 5. Some systematic deviations between experimental and calculated rates exist in Figs. 3 and 4; this may possibly be caused by model deficiency but it appears more likely that this is due to inaccuracy of the parameters of Table 3, which are average values resulting from the nonlinear regression analysis over a wide temperature range. Furthermore, at low carbon monoxide partial pressures the calculated rates are higher than the measured ones because pore diffusion as rate limiting factor could not be completely excluded under these conditions (compare Fig. 5).

The temperature dependence of the model parameters is given as an Arrhenius plot in Fig. 7. The symbols represent the constants resulting from fitting the kinetic data to Eq. (2) at one temperature only, whereas the straight lines are calculated from the model parameters in Table 3, which were determined by simultaneous fitting of all data obtained at all temperatures applied.

The formation of ethane was best approximated by:

$$r_{C_2H_6} = \frac{k'_{C_2H_4} K_C {}^2 p_{CO}}{(1 + K_C p_{CO}{}^{0.5} + K_H p_{H_2}{}^{0.5})^2} \quad (4)$$

The quality of this equation, however, is restricted since due to the low concentrations of ethane the analytical error was high. Therefore it should be only considered as an overall rate equation with no final significance with respect to the underlying mechanism, although some tentative mechanistic suggestions will be mentioned later.

The preexponential factor of the rate constant and the respective activation energy of Eq. (4) were obtained by simultaneous fitting of all kinetic data at all temperatures applied; for estimation the model parameters K_C, K_H, ΔH_C, and ΔH_H were used which had been previously derived for methane formation (compare Table 3). The relationship between the rates of ethane formation at 485 K and carbon monoxide partial pressure as experimentally determined (symbols) and calculated (solid lines) by Eq. (4) using the parameters of Table 3 is shown in Fig. 6. Agreement appears to be satisfactory, i.e., the general effects of carbon monoxide and hydrogen partial pressures are correctly presented.

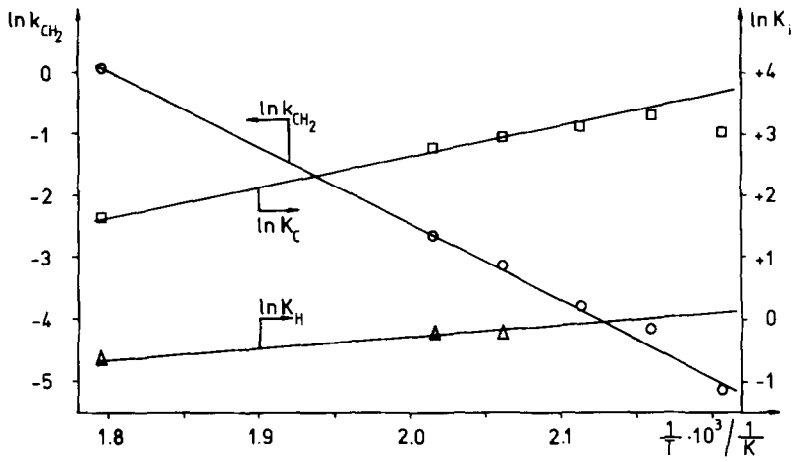

FIG. 7. Temperature dependence of model parameters of Eq. (2) (symbols show fitting of rate data at one temperature; lines show simultaneous fitting of all rate data at all temperatures).

DISCUSSION

Interpretation of the Kinetics of Methane Formation

The kinetics of carbon monoxide methanation according to Eq. (2) may be explained by the following reaction scheme:

(1) Carbon monoxide and hydrogen are dissociatively adsorbed and equilibrium is established; i.e., both processes are fast:

$$CO_g + 2^* \overset{K_{CO,D}}{\rightleftharpoons} C^* + O^* \qquad (I)$$

$$H_{2,g} + 2^* \overset{K_{H_2,D}}{\rightleftharpoons} 2H^* \qquad (II)$$

(2) Interaction of surface carbon and adsorbed hydrogen to a carbene species is the rate determining step (rds). Two reaction paths to the CH_2-surface intermediate, between which no discrimination is possible, may be considered:

(a) One surface carbon atom reacts simultaneously with two hydrogen atoms:

$$C^* + 2H^* \xrightarrow[\text{rds}]{k_{CH_2}} H_2C^* + 2^* \qquad (IIIa)$$

(b) Equilibrium is established between a carbine surface intermediate attached to two active sites and one surface hydrogen and one surface carbon atom:

$$C^* + H^* \overset{K_{CH}}{\rightleftharpoons} \underset{\cdot\ \ \cdot}{C\ldots H} \qquad (IIIb.1)$$
$$\ast \quad \ast$$

Then, the carbine species is further hydrogenated to CH_2, this being the rate determining step:

$$\underset{\cdot\ \ \cdot}{C\ldots H} + H^* \xrightarrow[\text{rds}]{k'_{CH_2}} H_2C^* + 2^* \qquad (IIIb.2)$$
$$\ast \quad \ast$$

(3) Subsequently, the carbene surface intermediate is quickly hydrogenated to methane, which easily desorbs. The reaction may be simplified as:

$$H_2C^* + 2H^* \xrightarrow{k_{CH_4}} CH_{4,g} + 3^* \qquad (IV)$$

(4) Surface oxygen reacts to water in a similar manner as reaction (IIIa):

$$O^* + 2H^* \xrightarrow{k_{H_2O}} H_2O_g + 3^* \qquad (V)$$

It is also conceivable that oxygen and hydrogen react alternatively in analogy to reactions (IIIb.1) and (IIIb.2). All steps are assumed to be fast.

On the basis of the above assumptions the kinetic Eq. (2) can be derived as explained in Appendix A. The above reaction

scheme is consistent with recent results on the mechanism of the formation of methane (*3–13*); it is always concluded that carbon monoxide as well as hydrogen are dissociatively adsorbed. However, no final conclusion with respect to the rate determining step can be drawn: Happel *et al.* (*5, 6*) suggested that either the hydrogenation of a C-, CH-, CH_2-, or CH_3-surface species may be rate determining; carbon and carbine are considered to be the most abundant surface intermediates (*6*). van Meerten *et al.* (*15*), who recently studied methanation on Ni/SiO_2, assumed that the interaction between a CH-surface intermediate and the adsorbed hydrogen atom is the slow step (model 15, Table 1). Also the present results suggest that either hydrogenation of surface carbon or of a CH-intermediate is the rate limiting step; however, the number of adsorption sites involved deviates from the proposal of van Meerten *et al.* (van Meerten: 2 sites; this work: 3 sites). The suggestions of Zagli *et al.* (*13*) and Dalla Betta and Shelef (*20*) that dissociation of carbon monoxide is rate limiting could not be confirmed; those proposals were definitely excluded under the conditions of this study.

Comparison of the Present Kinetics to Power Law Rate Equations

Frequently power law rate equations of the following form

$$r_{CH_4} = k_0 \exp(-E_{app}/RT) p_{CO}{}^n p_{H_2}{}^m \quad (5)$$

are used to describe the formation of methane (*2, 21, 22*). Generally, a positive value close or equal to unity has been found for m. However, negative as well as positive exponents for n have been mentioned, ranging between -1 and $+0.5$. The deviations in the reaction order with respect to carbon monoxide can be explained by the kinetics in this study. At high partial pressures of carbon monoxide and low temperatures the following relationship holds:

$$K_C p_{CO}{}^{0.5} \gg 1 + K_H p_{H_2}{}^{0.5}. \quad (6)$$

Hence rate Eq. (2) reduces to

$$r_{CH_4} = k_{CH_2} K_C{}^{-2} K_H{}^2 p_{CO}{}^{-1} p_{H_2} \quad (7)$$

At very high temperatures inhibition by adsorption of carbon monoxide and hydrogen can be neglected; the same is also true for low partial pressures of carbon monoxide and hydrogen. In both cases the denominator of Eq. (2) approaches 1; i.e., the rate equation reduces to:

$$r_{CH_4} = k_{CH_2} K_C K_H{}^2 p_{CO}{}^{0.5} p_{H_2} \quad (8)$$

At conditions when

$$K_H p_{H_2}{}^{0.5} \geq 1 + K_C p_{CO}{}^{0.5} \quad (9)$$

the reaction order with respect to hydrogen may become less than 1. Such a relationship has recently been reported by Sughrue and Bartholomew (*22*).

Interpretation of the Kinetics of Ethane Formation

Based upon the reaction scheme for the methanation of carbon monoxide the kinetics of the ethane formation according to Eq. (4) may be explained by rapid dimerization of two carbene species to an alkyl carbenic surface intermediate,

$$2H_2C^* \xrightarrow{k_{C_2H_4}} *[C_2H_4]^* \quad \text{(VI)}$$

which is subsequently hydrogenated to ethane:

$$*[C_2H_4]^* + 2H^* \xrightarrow{k_{C_2H_6}} C_2H_{6,g} + 4^* \quad \text{(VII)}$$

On this basis Eq. (4) can be derived as outlined in Appendix A. The proposed reaction scheme is consistent with results of Bell (*4*), Biloen *et al.* (*23*), and Rautavuoma and van der Baan (*19*). They assumed that the formation of olefins and higher paraffins occurs on Group VIII metals, which dissociatively adsorb carbon monoxide, by polymerization of surface hydrocarbons. Insertion of CH_2-species between a CH_3-group and metal as discussed by Bell (*4*) and Biloen *et al.* (*23*) could be excluded in this study by the above discussed dependence of the rate of ethane on partial pressures of

hydrogen and carbon monoxide. The same argument holds for a mechanism presented by Ponec (*3*) assuming insertion of carbon monoxide between a CH_2-group and the metal. Therefore, polymerization of CH_2-groups as suggested by Rautavuoma and van der Baan (*19*) seems to be a possible route to other hydrocarbons than methane. This view is supported by Brady and Pettit (*24*) who decomposed diazomethane in nitrogen on nickel and other transition metals and showed that the CH_2-species formed dimerised to ethylene.

Evaluation of Model Parameters

The activation energy of carbene formation as determined in this study amounts to 103 kJ/mol (see Table 3). Vannice (*2*), who investigated different supported nickel catalysts, reported values between 70 and 130 kJ/mol. This range is characteristic for methanation of carbon monoxide. Sughrue and Bartholomew (*22*) found a decrease in activation energy from 130 to 70 kJ/mol when increasing temperature from 473 to 623 K; the activation energy was derived from the temperature dependence of the rate constant of the general power law rate Eq. (5). The authors account for this effect by assuming a change in the reaction mechanism or the rate-limiting step. On the basis of the present results the change in activation energy can be explained without any of these assumptions. For low temperatures the kinetic Eq. (2) for the methanation of carbon monoxide reduces to the power law rate Eq. (7). Hence, for the apparent activation energy

$$E_{app} = E_{CH_2} - 2\Delta H_C + 2\Delta H_H \quad (10)$$

a value of 155 kJ/mol is obtained taking the data from Table 3. At very high temperatures Eq. (8) results. Therefore the apparent activation energy

$$E_{app} = E_{CH_2} + \Delta H_C + 2\Delta H_H \quad (11)$$

diminishes to 29 kJ/mol.

The true enthalpies of adsorption for dissociatively adsorbed hydrogen and carbon monoxide according to reactions (I) and (II) $\Delta H_{H_2,D}$ and $\Delta H_{CO,D}$ are related to the apparent enthalpies of adsorption ΔH_H and ΔH_C as well as to the activation energies of water formation E_{H_2O}, whose value could not be estimated by regression procedure, and of carbene formation E_{CH_2} of the model Eq. (2) in the following way (compare Eqs. (A10) and (A11) of Appendix A):

$$\Delta H_{H_2,D} = 2\,\Delta H_H \quad (12)$$

$$\Delta H_{CO,D} = 2\,\Delta H_C + E_{CH_2} - E_{H_2O} \quad (13)$$

Taking the data from Table 3 the heat of dissociative hydrogen adsorption $\Delta H_{H_2,D}$ is -32 ± 6 kJ/mol. The heat of dissociative carbon monoxide adsorption $\Delta H_{CO,D}$ can only be calculated if E_{H_2O} is known. The unknown value of E_{H_2O} was approximated as follows. For the reaction of gaseous hydrogen with oxygen adsorbed on a nickel surface Savchenko *et al.* (*25*) reported an activation energy $E_{app}(H_2O)$ of 54 kJ/mol at an oxygen surface coverage of 0.5. Assuming the above reaction scheme for the methanation of carbon monoxide, this value contains the heat of dissociative hydrogen adsorption (compare reactions (II) and (V)):

$$E_{app}(H_2O) = E_{H_2O} + \Delta H_{H_2,D} \quad (14)$$

The true activation energy of water formation E_{H_2O} depends now on $\Delta H_{H_2,D}$. Taking as lower limit -32 kJ/mol resulting from this work and as upper limit -66 kJ/mol measured by Wedler *et al.* (*26*) for dissociative adsorption of hydrogen on nickel at a surface coverage of 0.5, E_{H_2O} is estimated to be 103 ± 17 kJ/mol. Hence, taking the values of ΔH_C and E_{CH_2} from Table 3 the true heat of dissociative carbon monoxide adsorption resulting from Eq. (13) is -84 ± 25 kJ/mol, which value is clearly more exothermic than the one obtained for dissociative hydrogen adsorption. This is consistent with results from adsorption measurements (*26*) and calculations of enthalpies of adsorption on nickel (*27*).

CONCLUSIONS

In this study on the methanation of carbon monoxide a wide range of experimental conditions was covered. One rate equation resulted for the methanation reaction which was significantly better than others. For the respective kinetic model it is assumed that the reaction between surface carbon and two surface hydrogen atoms resulting from dissociatively adsorbed carbon monoxide and hydrogen to a carbene species is the rate-limiting step. The thermodynamic parameters of the model, i.e., the activation energy of CH_2 formation and the enthalpies of adsorption for carbon monoxide and hydrogen, are in agreement with other data known from the literature and obtained by other approaches. For the formation of ethane which is present as a minor by-product a tentative kinetic equation was derived by postulating that the CH_2-species dimerize to an alkyl carbenic surface intermediate, which is hydrogenated to ethane.

APPENDIX A

The rate equations for methane and ethane formation which have been found to be most significant to describe the kinetics of the two reactions are derived below.

(a) The reaction rates according to reactions (IIIa), (IV), (V), (VI), and (VII) depend on the degree of surface coverage by species *i:*

$$-r_{CO} = k_{CH_2}\theta_C\theta_H^2 \quad \text{(rds)} \tag{A1}$$

$$r_{CH_4} = k_{CH_4}\theta_{CH_2}\theta_H^2 \tag{A2}$$

$$r_{H_2O} = k_{H_2O}\theta_O\theta_H^2 \tag{A3}$$

$$r_{C_2H_6} = k_{C_2H_6}\theta_{C_2H_4}\theta_H^2 = k_{C_2H_4}\theta_{CH_2}^2 \tag{A4}$$

Assuming that the carbene formation via a carbine surface intermediate according to reactions (IIIb.1) and (IIIb.2) is valid, Eq. (A1) can be derived also from the following equations:

$$-r_{CO} = k'_{CH_2}\theta_{CH}\theta_H \quad \text{(rds)}$$

$$K_{CH} = \frac{\theta_{CH}}{\theta_C\theta_H}$$

(b) The equilibrium adsorption constants for carbon monoxide and hydrogen adsorption according to reactions (I) and (II) are given by:

$$K_{CO,D} = \frac{\theta_C\theta_O}{p_{CO}\theta_v^2} \tag{A5}$$

$$K_{H_2,D} = \frac{\theta_H^2}{p_{H_2}\theta_v^2} \tag{A6}$$

(c) The overall mass balance amounts to:

$$-r_{CO} = r_{CH_4} + 2r_{C_2H_6} = r_{H_2O} \tag{A7}$$

(d) Surface coverage of oxygen and carbene results from Eqs. (A1), (A2), and (A3) neglecting the ethane formation in (A7), i.e., if

$$-r_{CO} = r_{H_2O} \simeq r_{CH_4}$$

is valid:

$$\theta_O = \frac{k_{CH_2}}{k_{H_2O}}\theta_C \tag{A8}$$

$$\theta_{CH_2} = \frac{k_{CH_2}}{k_{CH_4}}\theta_C \tag{A9}$$

(e) Surface coverage of carbon and hydrogen atoms is obtained from Eqs. (A5), (A6), and (A8):

$$\theta_C = K_C p_{CO}^{0.5}\theta_v$$

$$K_C = \left(\frac{k_{H_2O}}{k_{CH_2}}K_{CO,D}\right)^{0.5} \tag{A10}$$

$$\theta_H = K_H p_{H_2}^{0.5}\theta_v$$

$$K_H = (K_{H_2,D})^{0.5} \tag{A11}$$

(f) The surface balance can be approximated assuming only adsorbed carbon, hydrogen atoms, and vacant sites on the catalyst and neglecting the coverage by oxygen and hydrocarbons:

$$1 \simeq \theta_v + \theta_C + \theta_H \tag{A12}$$

(g) Surface coverage of vacant sites is calculated from (A10) to (A12):

$$\theta_v = \frac{1}{1 + K_C p_{CO}^{0.5} + K_H p_{H_2}^{0.5}} \tag{A13}$$

(h) Then the rate Equation (2) of methane

formation results from combination of (A1) with Eqs. (A10), (A11), and (A13) keeping in mind that $-r_{CO} \simeq r_{CH_4}$ is valid. The kinetic Eq. (4) of ethane formation is obtained by combining Eq. (A4) with Eqs. (A9), (A10), and (A13). Thereby the rate constant $k'_{C_2H_4}$ is defined as follows:

$$k'_{C_2H_4} = k_{C_2H_4} \left(\frac{k_{CH_2}}{k_{CH_4}}\right)^2 \qquad \text{(A14)}$$

APPENDIX B: NOMENCLATURE

E	activation energy, kJ/mol
k	reaction rate constant, variable
K	adsorption constant, variable
p	partial pressure, bar
r	reaction rate, mol/h g-catalyst
T	reaction temperature, K
ΔH	enthalpy of adsorption, kJ/mol
θ	degree of surface coverage
*	vacant surface site

Indices

app	apparent
D	dissociation
g	gas phase
v	vacant

ACKNOWLEDGMENT

This investigation was supported by a grant of the Minister for Research and Technology of the Federal Republic of Germany.

REFERENCES

1. Vlasenko, V. M., Yuzefovich, G. E. *Russ. Chem. Rev.* **38,** 728 (1969).
2. Vannice, M. A., *Catal. Rev.—Sci. Eng.* **14,** 153 (1976).
3. Ponec, V., *Catal. Rev.—Sci. Eng.* **18,** 151 (1978).
4. Bell, A. T., *Catal. Rev.—Sci. Eng.* **23,** 203 (1981).
5. Happel, J., Suzuki, I., Kokayeff, P., and Fthenakis, V., *J. Catal.* **65,** 59 (1980).
6. Happel, J., Cheh, H. Y., Otarod, M., Ozawa, S., Severdia, A. J., Yoshida, T., and Fthenakis, V., *J. Catal.* **75,** 314 (1982).
7. McCarty, J. G., and Wise, H., *J. Catal.* **57,** 406 (1979).
8. Goodman, D. W., Kelley, R. D., Madey, T. E., White, J. M., *J. Catal.* **64,** 479 (1980).
9. Goodman, D. W., Kelley, R. D., Madey, T. E., and Yates, J. T., *J. Catal.* **63,** 226 (1980).
10. Gardner, D. C., and Bartholomew, C. H., *Ind. Eng. Chem. Fundam.* **20,** 229 (1981).
11. Rabo, J. A., Risch, A. P., and Poutsma, M. L., *J. Catal.* **53,** 295 (1978).
12. Wentrcek, P. R., Wood, J. B., and Wise, H. *J. Catal.* **43,** 363 (1976).
13. Zagli, A. E., Falconer, J. L., and Keenan, C. A., *J. Catal.* **56,** 453 (1979).
14. Klose, J., dissertation, Ruhr-Universität Bochum, 1982.
15. van Meerten, R. Z. C., Vollenbrock, J. G., De Croon, M. H. J. M., Van Nisselroy, P. F. M. T., and Coenen, J. W. E., *Appl. Catal.* **3,** 29 (1982).
16. Bard, Y., "Nonlinear Parameter Estimation." Academic Press, New York, 1974.
17. Himmelblau, D. M., "Process Analysis by Statistical Methods." Wiley, New York, 1970.
18. Satterfield, C. N., "Mass Transfer in Heterogeneous Catalysis" Colonial Press Inc., Clinton, Massachusetts, 1977.
19. Rautavuoma, A. O. I., and van der Baan, H. S., *Appl. Catal.* **1,** 247–272 (1981).
20. Dalla Betta, R. A., and Shelef, M., *J. Catal.* **49,** 383 (1977).
21. Takahashi, N., Shimazaki, Y., and Yashimi, T., *Z. Phys. Chem. NF* **118,** 221 (1979).
22. Sughrue, E. L., and Bartholomew, C. H., *Appl. Catal.* **2,** 239 (1982).
23. Biloen, P., Helle, J. N., and Sachtler, W. M. H., *J. Catal.* **58,** 95 (1979).
24. Brady, R. C. III, and R. Pettit, *J. Amer. Chem. Soc.* **102,** 6182 (1980).
25. Savchenko, V. I., Boreskov, G. K., and Dadayan, K. A., *Kinet. Katal.* **20,** 610 (1979) [in English].
26. Wedler, G., Papp, H., and Schroll, G., *J. Catal.* **38,** 153 (1975).
27. Miyazaki, E., *J. Catal.* **65,** 84 (1980).